



**HAL**  
open science

## Deactivation by coking of industrial ZSM-5 catalysts used in LDPE pyrolysis and regeneration by ozonation process – Bench scale studies

V. Daligaux, Romain Richard, Marin Gallego Mylène, Valérie Ruaux, Ludovic Pinard, Marie-Hélène Manero

### ► To cite this version:

V. Daligaux, Romain Richard, Marin Gallego Mylène, Valérie Ruaux, Ludovic Pinard, et al.. Deactivation by coking of industrial ZSM-5 catalysts used in LDPE pyrolysis and regeneration by ozonation process – Bench scale studies. *Applied Catalysis A: General*, 2024, 671, pp.119581. 10.1016/j.apcata.2024.119581 . hal-04594805

**HAL Id: hal-04594805**

**<https://hal.science/hal-04594805>**

Submitted on 17 Jun 2024

**HAL** is a multi-disciplinary open access archive for the deposit and dissemination of scientific research documents, whether they are published or not. The documents may come from teaching and research institutions in France or abroad, or from public or private research centers.

L'archive ouverte pluridisciplinaire **HAL**, est destinée au dépôt et à la diffusion de documents scientifiques de niveau recherche, publiés ou non, émanant des établissements d'enseignement et de recherche français ou étrangers, des laboratoires publics ou privés.



Distributed under a Creative Commons Attribution 4.0 International License



# Deactivation by coking of industrial ZSM-5 catalysts used in LDPE pyrolysis and regeneration by ozonation process – Bench scale studies

V. Daligaux<sup>a</sup>, R. Richard<sup>a,\*</sup>, M. Marin-Gallego<sup>a</sup>, V. Ruaux<sup>b</sup>, L. Pinard<sup>b</sup>, M.-H. Manero<sup>a</sup>

<sup>a</sup> Laboratoire de Génie Chimique, Université de Toulouse, CNRS, INPT, UPS, F-31030 Toulouse, France

<sup>b</sup> Laboratoire Catalyse et Spectrochimie, ENSICAEN, UNICAEN, CNRS, F-14050 Caen, France

## ARTICLE INFO

### Keywords:

Coke deactivation  
Plastics pyrolysis  
Ozone catalyst regeneration  
Pilot-scale  
Studies  
Zeolite characterization

## ABSTRACT

Study of the catalytic deactivation during successive uses of ZSM-5 catalysts in bench-scale pyrolysis of low-density polyethylene (200:20 g LDPE:ZSM-5) has been carried out in a semi-batch reactor at 450 °C. The correlation between coke formation over catalyst properties and selectivity during pyrolysis is observed. The loss of catalytic performances translates into a significant drop of aromatics and an increase of waxes in pyrolysis products. The observed deactivation is due to the formation of heavy coke over the catalysts, causing surface hindering, porosity blockage and acid sites diminution. The capacity of ozonation process to regenerate such coked catalysts around 100 °C is demonstrated using a fixed bed reactor. Different times of exposure are investigated to evaluate ozonation efficiency. By using this coke oxidizing treatment during 48 h, regenerated catalysts recovered their initial textural and chemical characteristics (porous volume and acidity) as well as their catalytic performances (similar aromatics proportion as the first pyrolysis).

## 1. Introduction

Global plastic waste production has been exploding during the last decades due to the extensive use of plastics in our daily lives. Only approximately 20% of generated plastic waste is recycled while the rest is either discarded, incinerated or mismanaged [1]. Developing new recycling processes to support the existing methods, consisting mostly in mechanical recycling, is therefore of high importance to mitigate plastic pollution and develop closed-loop recycling. Many chemical methods have been investigated for the revalorization of plastic waste into valuable products [2]. Among them, pyrolysis allows the conversion of polymers into oils and base chemicals which can be used as fuels or feedstock for chemical industry [3]. Use of catalysts in this process allows the formation of high-value products at lower temperatures compared to thermal pyrolysis, due to their cracking and rearrangement properties [4]. The industrial development of plastics catalytic pyrolysis is considered by using reactor configurations allowing continuous plastic feed, such as fluidized and circulating bed, screw kiln or spouted bed reactors [5–7]. Different catalytic materials, such as fluid catalytic cracking (FCC) catalysts or zeolites, were investigated over the years to study their impact on pyrolysis reactivity and selectivity [8–10]. Zeolite catalysts have been intensively investigated as their wide range of

geometries and acidity strength provide a great number of possibilities in terms of obtainable products based on used feedstock. Among them, ZSM-5 zeolites have been identified in the literature as an efficient catalyst for pyrolysis as their properties promote the formation of molecules of higher interest [11]. However, industrial use of catalytic pyrolysis remains restrained by an important coke formation over the catalyst, leading to a rapid decrease of catalyst performances and products quality [12]. Deactivation via coking consists in formation of carbonaceous deposits, causing gradual surface hindering and porosity blockage, leading to the diminution of accessible active sites and therefore to loss of catalytic activity [13,14]. Despite heavy investigation over the years, coke formation remains a very challenging phenomenon due to the complexity and diversity of coke molecule structures. Mechanisms of coke formation and growth are known to form light aliphatic coke (ratio H/C > 1) at moderate temperature, turning into heavy polyaromatic clusters (ratio H/C < 1) via condensation when longer exposed or at high temperatures [13,14]. Many works intended to study coke formation during pyrolysis with various catalysts and kind of reactors in order to mitigate coking, but the deactivation remains present and leads to a relatively quick loss of catalyst performances [15]. Therefore, the viability of catalytic pyrolysis is driven by the possibility of reusing coked catalysts several times

\* Corresponding author.

E-mail address: [romain.richard@iut-tlse3.fr](mailto:romain.richard@iut-tlse3.fr) (R. Richard).

<https://doi.org/10.1016/j.apcata.2024.119581>

Received 8 November 2023; Received in revised form 17 January 2024; Accepted 18 January 2024

Available online 20 January 2024

0926-860X/© 2024 The Author(s). Published by Elsevier B.V. This is an open access article under the CC BY license (<http://creativecommons.org/licenses/by/4.0/>).

keeping acceptable/exploitable products but also of regenerating the catalysts to recycle them. Indeed, deactivation via coking is reversible in most cases and catalytic properties and activity can be recovered with different processes.

For combined economic and environmental concerns, regeneration processes were developed in order to be able to reuse deactivated catalysts, which are often produced from rare and/or expensive materials [16]. While coke oxidation with air or oxygen is the most-used process at industrial scale nowadays to remove coke, other methods such as gasification or hydrogenation can be found [17]. Different papers investigated the regeneration and reuse of catalysts coked during pyrolysis, using the “classical” process of coke combustion with oxygen over 400 °C, and proved that catalytic activity could successfully be recovered after coke oxidation [18–20]. However, this process presents important limitations because of its important energy consumption and severe operating conditions that might degrade thermo-sensitive catalysts. Some recent studies are focusing on the development of alternative methods, such as advanced oxidation processes (AOPs), to achieve coke removal and catalytic activity recovery with higher efficiency and lower energy consumption in milder conditions [21,22]. Due to its recent interest, very limited data can be found in the literature concerning regeneration of coked catalysts using AOPs [23–25]. The ability of these processes to restore catalytic activity is the main objective of these studies so far and their energetic viability compared to combustion remains to be investigated. Among these methods, ozonation presented promising results in terms of coke removal around 100 °C [23]. On top of the reduced temperature, such conditions are interesting for catalysts regeneration to maintain catalytic structure and mitigate the apparition of hot spots, which can lead to dealumination and depopulation of acid sites over zeolites or other structural changes over more thermosensitive materials [26]. However, few studies were found in which ozonated catalysts are reused in initial process [27]. The objective of this work is to investigate the capacity of the ozonation process to restore catalytic activity at lower temperatures after deactivation with coke formation during pyrolysis. In this work, ZSM-5 industrial catalysts are recycled after regeneration via ozonation in order to compare their activity with the fresh catalysts.

This work is embedded in the combined logic of development of new catalytic processes answering to contemporary issues and circular economy with catalytic material recycling. This study investigates the deactivation and regeneration of catalytic material involved in innovative processes: a deep comprehension of coke formation during pyrolysis is achieved through analysis of liquid products and characterization of solid catalysts, before investigating the regeneration efficiency of ozonation as an innovative method for coke removal. The authors identified catalytic pyrolysis of plastics in the literature as an easy-to-use reaction allowing revalorization of plastic wastes which main drawback is the important deactivation by coking [28,29]. Up to now, most of the studies related to catalytic deactivation during pyrolysis of plastics are limited to a single use of spent catalysts in the reaction. The aim of this work is to reuse spent industrial catalysts more than once to reach a better understanding of coke formation during pyrolysis and to conclude about the eventual possibility to reuse extensively spent catalysts before removing it for regeneration. Díaz et al. conducted similar study on coke deactivation over HZSM-5 catalysts during oligomerization reaction, followed by regeneration by coke combustion with air [30]. Use of ozonation as an alternative method for coke removal intends to assess catalytic recovery comparatively to classic coke oxidation conducted in most studies. Such work aims to demonstrate the regenerating capacity of ozonation prior to consider its energetic viability compared to combustion in future investigations. Use of ozone indeed generates other costs despite lowered temperatures: complete process energetic analysis needs to be conducted to determine the industrial relevance of ozonation. Different analytical techniques were used to characterize fresh, spent and regenerated samples, such as elemental analysis, N<sub>2</sub> adsorption/ desorption, FTIR-Pyridine or <sup>13</sup>C NMR, in order to provide a

complete overview of coke deposition and its influence over textural and chemical properties of zeolite. Their corresponding catalytic efficiency is evaluated by a semi-quantitative GC-MS analysis of pyrolysis products.

## 2. Material and methods

### 2.1. Materials

Plastic feedstock used during the pyrolysis experiments is virgin low-density polyethylene (LDPE) provided by Sigma-Aldrich. Catalytic material used during the experiments are commercial HZSM-5 provided by Tosoh Company. Characteristics and properties of polyethylene and catalysts used during the experiments are presented in Table 1. The proportion of alumina binder in the industrial catalysts was determined by NMR of <sup>27</sup>Al and <sup>29</sup>Si. The Si/Al ratio value of diluted zeolites being 18 against 23 for pure crystals, binder proportion is estimated around 22%. Catalysts and polyethylene are used as received in their initial form without further preparation step. For all the experiments, polyethylene and catalysts are loaded in the reactor at ambient temperature.

### 2.2. Experimental setups and procedures

The catalytic pyrolysis experiments were carried out in a semi-batch reactor (2 L capacity). The experimental setup scheme is presented in Fig. 1. During a typical experiment, 200 g of polyethylene were loaded in the reactor with 20 g of catalysts. This 10:1 mass ratio is identified in the literature as a commonly used value, and therefore integrated in our protocol [19,31]. In this work, plastics and zeolite were loaded in the reactor in layers (symbolized by the letter “L”): polyethylene and catalysts are placed in four successive layers of 50 g LDPE/ 5 g ZSM-5. After sealing the reactor and inerting the atmosphere with nitrogen at 2 L min<sup>-1</sup>, sweeping is turned off and the reactor is heated up to 450 °C during 40 min with electric resistances in shelves. The current regulation implies an important heating rate of 40 °C/min and an overshoot of 30 °C: maximal temperature is therefore 480 °C before stabilization at 450 °C after 20 min. Most of the polyethylene degradation occurs around 30 min of pyrolysis. After 40 min of heating, N<sub>2</sub> circulation is turned back on to sweep the decomposition components remaining in the reactor. The gases formed during the catalytic cracking, after going through another 2 L volume cylinder, referred as rearrangement level later on, flow through two successive condensation stages connected by insulated stainless steel tubing (4 mm internal diameter). The cooling-down temperatures at the two stages are respectively 80 °C (water) and 0 °C (ethylene glycol). The condensed vapors are subsequently collected as pyrolysis waxes and oils for analysis, while the uncondensed gases are evacuated to extraction. After appropriate waiting time for cool down (around 8 h), used catalysts are recovered and collected for characterization. No other solid residues are observed except coked catalysts meaning that polyethylene is entirely degraded.

**Table 1**  
Properties of industrial catalysts and plastics.

Catalysts ZSM-5: HSZ-822HOD1A (Tosoh). Lot n°TZ-200805.	
Binder	Alumina
Shape	Extrudate
Size (diameter x length) (mm)	1.5 × 2-6
Bulk density (kg/m <sup>3</sup> )	680
Grain density (kg/m <sup>3</sup> )	~ 1300
Alumina binder proportion (%)	22
Zeolite powder SiO <sub>2</sub> /Al <sub>2</sub> O <sub>3</sub> (mol/mol) Na <sub>2</sub> O (wt%)	23 0.05
Polyethylene (LDPE) Product n°428043 (Sigma-Aldrich)	
CAS number	9002-88-4
Shape	Pellets
Size (diameter) (mm)	4-5
Material density (kg/m <sup>3</sup> )	925

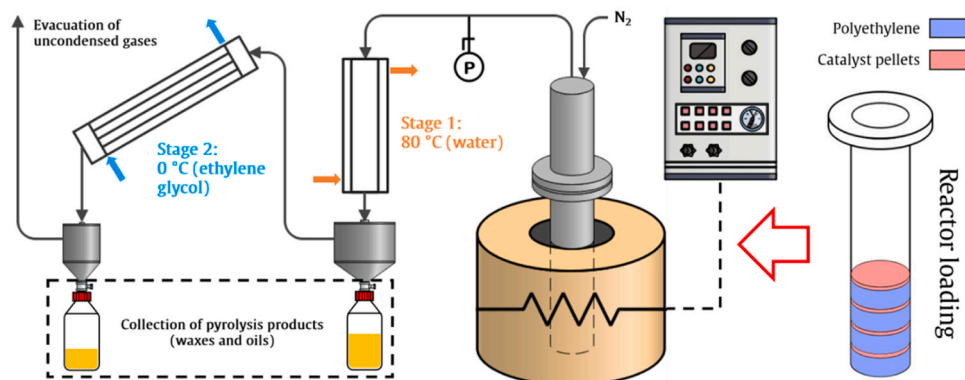


Fig. 1. Scheme of experimental setup for pyrolysis and illustration of the loading method in layers.

Thermal pyrolysis experiment is conducted using identical conditions without catalysts for comparison.

The regeneration of spent catalysts is carried out in another experimental set-up implementing a fixed-bed tubular glass reactor with a 10 g capacity (14 mm internal diameter, 90 mm catalytic bed height). Therefore, the 20 g of coked zeolites previously collected are regenerated in two separate runs using identical conditions. The ozonation setup is presented in previous work using a different reactor configuration with smaller capacity [32]. The catalytic bed is exposed to an ozone gas flow (50–60 g/Nm<sup>3</sup> at 100 L/h) at 100 °C. Different times of exposition are investigated from 8 to 48 h. Ozone is generated onsite thanks to a lab-scale ozoner (Trailigaz Labo 76 50 Hz) from pure and dry oxygen (B50 Linde, purity > 99.5 vol%). After characterization, ozonated catalysts are reused in a new pyrolysis run without any pretreatment or reactivation step.

### 2.3. Analytical techniques

#### 2.3.1. Pyrolysis oils characterization and catalytic performance

Liquid fractions of pyrolysis oils are analyzed by gas chromatograph coupled with mass spectrophotometry (GC-MS). To complete determination of chemical composition, gas chromatograph Thermo Trace 1300 is used coupled with a TSQ 8000 Evo quadrupole detector. The GC is equipped with a capillary column of dimensions 30 m long, 0.25 mm internal diameter and 1.4 μm thickness of diphenyl/dimethyl polysiloxane film (Rtx-502.2). Samples are diluted in heptane with a 1:20 vol ratio before analysis. The initial oven temperature is 40 °C and is increased up to 150 °C (24 °C.min<sup>-1</sup> ramp, held 1 min), then to 250 °C (12 °C.min<sup>-1</sup> ramp, held 20 min). The split injection temperature is applied at 250 °C. The transfer line and ion source temperatures are 240 °C and 250 °C respectively. Mass data is acquired in full-scan mode between 30 and 600 *m/z*. Molecules are attributed to corresponding peak using NIST database.

No quantitative information is collected during the experiments as the current version of the experimental setup does not allow to determine pyrolysis yields and complete material balance. Catalytic efficiency is therefore measured by following the evolution of pyrolysis condensed products nature. Proportion of aromatics and fractions of molecules according to their number of carbons in the oils are used as a descriptor of catalytic performance during pyrolysis. The term of catalytic selectivity is consequently preferred to catalytic activity in this work. The repeatability of this method and indicators was confirmed by conducting different pyrolysis experiments with fresh catalysts in identical conditions. Based on this study, the experimental error related to aromatics proportion is ± 5% and ± 2% for the repartition between the different fractions. The indicated values for the composition of pyrolysis products, for spent and regenerated catalysts, are considered to be embedded in this interval of confidence.

#### 2.3.2. Catalysts characterization

Textural properties of fresh, deactivated and regenerated catalyst samples are obtained with N<sub>2</sub>-adsorption under vacuum (10<sup>-4</sup>–10<sup>-5</sup> Pa) at – 196 °C using a BELSORP-Max apparatus (BEL Japan). From the complete adsorption isotherms, main results are determined based on different methods. Brunauer-Emmet-Teller (BET) equation is used for surface area and global porosity. Microporous volume data is obtained by Horvath-Kawazoe (HK) method [33]. Mesoporous volume is determined as the difference between total porosity and microporous volume.

Acidic properties of catalysts are analyzed with FTIR spectroscopy using pyridine as probe molecule. Samples are pressed (10<sup>9</sup> Pa) into self-supported discs (2 cm<sup>2</sup> area, 7–10 mg.cm<sup>-2</sup>) and placed in a quartz cell equipped with KBr windows. A movable quartz sample holder permitted adjustment of the pellet in the infrared beam for spectral acquisition and placement into a furnace at the top of the cell for thermal treatments. The cell is connected to a vacuum line for evacuation, calcination steps (P residual: 10<sup>-3</sup>–10<sup>-4</sup> Pa) and for the introduction of probe molecules (pyridine vapour phase at 150 °C). Spectra are recorded at room temperature in the 4000–400 cm<sup>-1</sup> range, with 4 cm<sup>-1</sup> resolution, on a Nicolet Nexus spectrometer equipped with an extended KBr beam splitting device and a detector for Fourier transform spectroscopy (DTGS). Quantification of both Brønsted and Lewis acid sites is determined by integration of IR spectra bands and by using molar absorption coefficients of pyridine commonly accepted in literature: 1.67 cm.μmol<sup>-1</sup> for the Brønsted sites band (1545 cm<sup>-1</sup>) and 2.22 cm.μmol<sup>-1</sup> for the Lewis sites band (1455 cm<sup>-1</sup>) [34].

#### 2.3.3. Coke quantity and nature

Elemental analysis of coked samples is performed by combustion at 1100 °C using Perkin Elmer 2400 Series II Flash Combustion Analyzer to determine the carbon and hydrogen content. The results, given in weight percentage with a ± 0.1 wt% precision, are used as indicator of deposited coke as it is the only source of carbon in the samples.

Comprehensive insight of coke molecules nature and structure is given by the exploitation of solid-state <sup>13</sup>C cross-polarization magic-angle spinning (CP-MAS) NMR analysis. Spectra are recorded at ambient temperature in a Bruker Avance III HD 400 (9.4 T) spectrometer. Samples are placed in 4 mm zirconia rotors with a MAS rotation speed of 10 kHz. Quantitative acquisition is made with 10 periods of cross-polarization with a contact time of 1.1 ms separated with a repolarizing time <sup>1</sup>H of 0.5 s [35]. The recycling time is set at 1.5 s. The carbon species present over the coked zeolites are identified with a simplified multi Gaussian deconvolution (6 peaks). Each chemical shift is attributed based on literature research to particular carbon environment [36–38]. Integration data of the deconvoluted peaks are used to determine their respective proportions and condensation degree similarly to Chen *et al.* work [39]. Data is normalized based on carbon content obtained by elemental analysis to have a quantitative approximation.

### 3. Results and discussion

#### 3.1. Catalytic deactivation during pyrolysis

In order to study the evolution of deactivation and progressive formation of coke during pyrolysis, experiments were performed in five successive runs where catalysts are reused without any intermediate treatment. Analysis of pyrolysis products and used catalysts is performed after each run. As mentioned in Section 2.2, the bed of catalysts and LDPE pellets are initially structured by alternating layers (labelled L). Coked catalysts indicated as L' and L'' are experiments conducted with identical conditions to study the repeatability of coking during catalytic pyrolysis. The number added after this indicative letter corresponds to the number of reuses in pyrolysis. As an example, L4 experiment is the fourth reuse of ZSM-5 catalysts in pyrolysis. Collected samples (spent catalysts and pyrolysis products) are named after this experiment indicator.

##### 3.1.1. Evolution of pyrolysis products selectivity

The compositions of pyrolysis products collected after the first condenser (Stage 1 on Fig. 1) are presented in Table 2 for the successive experiments (L1 to L4). Wax and oil fraction are there collected as a unique homogeneous phase at 80 °C, which then turns solid by cooling down until ambient temperature. Proportion of aromatics and fractions of molecules according to their number of carbons are used as a descriptor of catalytic performance in the oils during pyrolysis. Peak area percentages were extracted from the total chromatogram to determine the distribution of the products. The different fractions of obtained molecules are sorted as follows: C7 to C9, corresponding to gasoline, C10 to C14, representing kerosene components, and C15 + molecules, often mentioned in the literature as heavy oils or waxes [40]. The proportion of aromatics is also presented for each fraction as well as the main products of interest: toluene and xylenes. Complete list of identified products during pyrolysis using fresh catalysts is provided in supporting information with corresponding peak area.

Compared to thermal pyrolysis of plastics, the addition of catalysts is known to enhance the cracking of polymers and to allow the formation of aromatic products via mechanisms of rearrangement, cyclization and H-transfer [41,42]. The use of ZSM-5 zeolites has been extensively studied due to their shape selectivity leading to the important formation of light products and aromatics [43]. Such behavior is confirmed in this study as the fraction of light oil (C7-C9) and aromatics is more important using fresh catalysts compared to thermal pyrolysis [4,19]. Thermal pyrolysis only presents 0.2% of aromatics and 40.1% of C7-C9 molecules, while same experiment with fresh zeolites presents aromatics proportion of 91.9%, and a light oil fraction (C7-C9) of 94.9%. Aromatics formed during pyrolysis of polyethylene are mainly molecules containing 7 or 8 carbon atoms, therefore part of the aforementioned light fraction. No aromatic products are identified in the wax fraction (C15 +). As observed in Table 2, the repartition of obtained pyrolysis

products changes during the successive reuses of catalysts. The total proportion of aromatics decreases drastically, from 91.9% to 27.5% after five successive pyrolysis reuses. This evolution traduces the progressive loss of catalytic performances, and especially the diminution of zeolite rearrangement capacity. The cracking potential of ZSM-5 is also affected by this decrease of catalytic performance as lower concentrations of light oil products (C7-C9) is formed after successive reuses while the proportion of kerosene products (C10-C14) increases. The carbon-number distribution of molecules obtained during pyrolysis is a typical indicator of catalytic performances for cracking [44]. A shift towards higher carbon number is usually obtained when catalytic activity decreases [31]. An important decrease of the light fraction (C7-C9) is indeed observed during the five successive reuses as its proportion drops from 94.9% to 69.8%. The evolution of monocyclic molecules content in this fraction is mostly responsible of the global decrease of aromatic products as an important loss of toluene and xylenes production is observed. After the fifth catalysts reuse, the nature of obtained products remains quite different from the composition of thermal pyrolysis oils, suggesting that catalysts remain chemically active despite an important loss of initial selectivity.

##### 3.1.2. Influence of coking on catalysts characteristics

Textural and chemical properties of spent catalysts are given in Table 3 alongside the evolution of carbon content and H/C ratio during successive pyrolysis. These samples correspond to the used ZSM-5 catalysts collected after each pyrolysis run presented in Section 2.1.1. The properties are compared to fresh industrial ZSM-5 characteristics to evaluate deactivation caused by coke deposition.

The formation of coke is illustrated by the apparition of carbon on the catalysts with an increasing content as zeolites are reused and further deactivated. Carbon content is expected to increase after each reuse, but a different tendency appears. Whereas carbon content reaches 8.2 wt% after a single pyrolysis run (L1), its value fluctuates around 9 wt% with a maximum of 10.3 wt% from the second to the fifth use. As

**Table 3**

Textural and chemical properties of fresh and spent catalysts after successive runs of pyrolysis.

Property	Fresh	L1	L2	L3	L4	L5
Carbon content (wt%)	-	8.2	6.5	8.3	10.3	9.9
Hydrogen content (wt%)	-	1.0	0.6	0.4	0.7	0.4
H/C ratio (mol/mol)	-	1.6	1.1	0.6	0.8	0.5
BET surface area (m <sup>2</sup> .g <sup>-1</sup> )	369.6	231.7	138.9	49.1	42.6	43.3
Total pore volume (cm <sup>3</sup> .g <sup>-1</sup> )	0.38	0.29	0.23	0.13	0.18	0.16
Microporous volume V <sub>micro</sub> (cm <sup>3</sup> .g <sup>-1</sup> )	0.17	0.11	0.07	0.03	0.02	0.02
Mesoporous volume V <sub>meso</sub> (cm <sup>3</sup> .g <sup>-1</sup> )	0.21	0.18	0.16	0.10	0.16	0.14
Brønsted acid sites (μmol.g <sup>-1</sup> )	294	191	103	31	10	4
Lewis acid sites (μmol.g <sup>-1</sup> )	193	76	66	33	27	25

**Table 2**

Composition of pyrolysis fractions analyzed by GC-MS using spent and regenerated catalysts.

Condensed products distribution (%)	Thermal	Fresh	L1	L2	L3	L4	R8	R48
Identified	96.5	98.5	97.4	95.0	93.6	95.0	95.9	96.6
Aromatics (± 5%)	0.2	91.9	77.3	55.8	30.6	27.5	78.7	91.4
C7-C9 (Gasoline, ± 2%)								
Total	40.1	94.9	88.8	77.2	69.5	69.8	87.9	92.2
Aromatics	0.0	91.5	76.6	55.5	30.6	27.4	78.2	89.6
C10-C14 (Kerosene, ± 2%)								
Total	38.2	3.1	8.0	15.8	20.4	23.1	6.1	3.3
Aromatics	0.2	0.4	0.7	0.3	n.d.	n.d.	0.5	1.8
C15 + (Heavy oils)								
Total	18.2	0.5	0.7	2.0	3.6	2.1	1.9	1.2
Main products								
Toluene	-	26.8	28.8	20.8	17.1	15.4	15.3	18.5
Xylenes	-	59.4	40.4	26.5	8.2	6.3	52.1	61.8



illustrated on Fig. 2, carbon deposition and coke formation greatly affect specific surface area, global porosity and acid sites concentration. The evolution of total porosity takes into account the diminution of both meso- and micro-pores volumes. Microporosity is the most impacted with a 90% loss after five successive uses (compared to 33% diminution for mesoporosity). This difference is due to the various deactivating pathways: on top of coke micropore volume occupancy, micropores are also subject to pore blocking. The location of carbon deposits formed during pyrolysis are furtherly discussed in Section 2.1.3.

The evolution of acidity is decreasing accordingly to the textural properties: Brønsted sites, mostly located in zeolite microporosity, is heavily impacted with a 99% loss after five pyrolysis. Due to their high reactivity, Brønsted sites are subject to important deactivation as coke precursors are susceptible to react over such acid sites [45]. On the other hand, Lewis sites are little impacted as they are mostly located on the external surface of the crystals and alumina binder, thus in mesopores [46]. Brønsted sites are known to be the most chemically reactive locations during pyrolysis, for either molecule aromatization (H-transfer) but also cracking (protolytic mechanism), while Lewis acidity only promotes cracking ( $\beta$ -scission) at a lower extent [43,47]. The important loss of Brønsted sites is correlated with the decrease of aromatics proportion in the pyrolysis oils (Section 2.1.1) while the smaller diminution of Lewis sites explains the mitigated decrease of cracking performances. Despite complete loss of Brønsted acidity after the fifth experiment, catalysts remain chemically active as products remain different from thermal pyrolysis. Further reuse of the catalysts is expected to lead to a complete deactivation, where catalysts become chemically inert.

In order to investigate the influence of coke deposits over catalytic characteristics, the evolution of main properties is plotted as a function of carbon load in Fig. 3(a, b). All the aforementioned samples are here presented as well as L' and L' repeatability experiments. As expected from typical deactivation behavior, a gradual loss of both microporous volume and acidity with carbon load increase is observed. While most of the points are embedded in a linear correlation, carbon content is

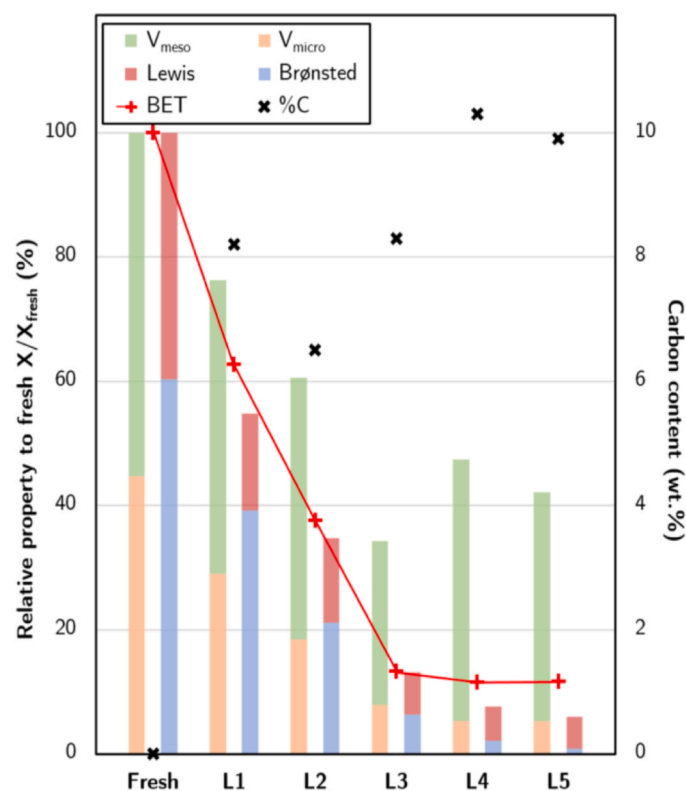


Fig. 2. Evolution of catalysts textural and chemical properties due to coke deposition during several successive runs of pyrolysis of LDPE.

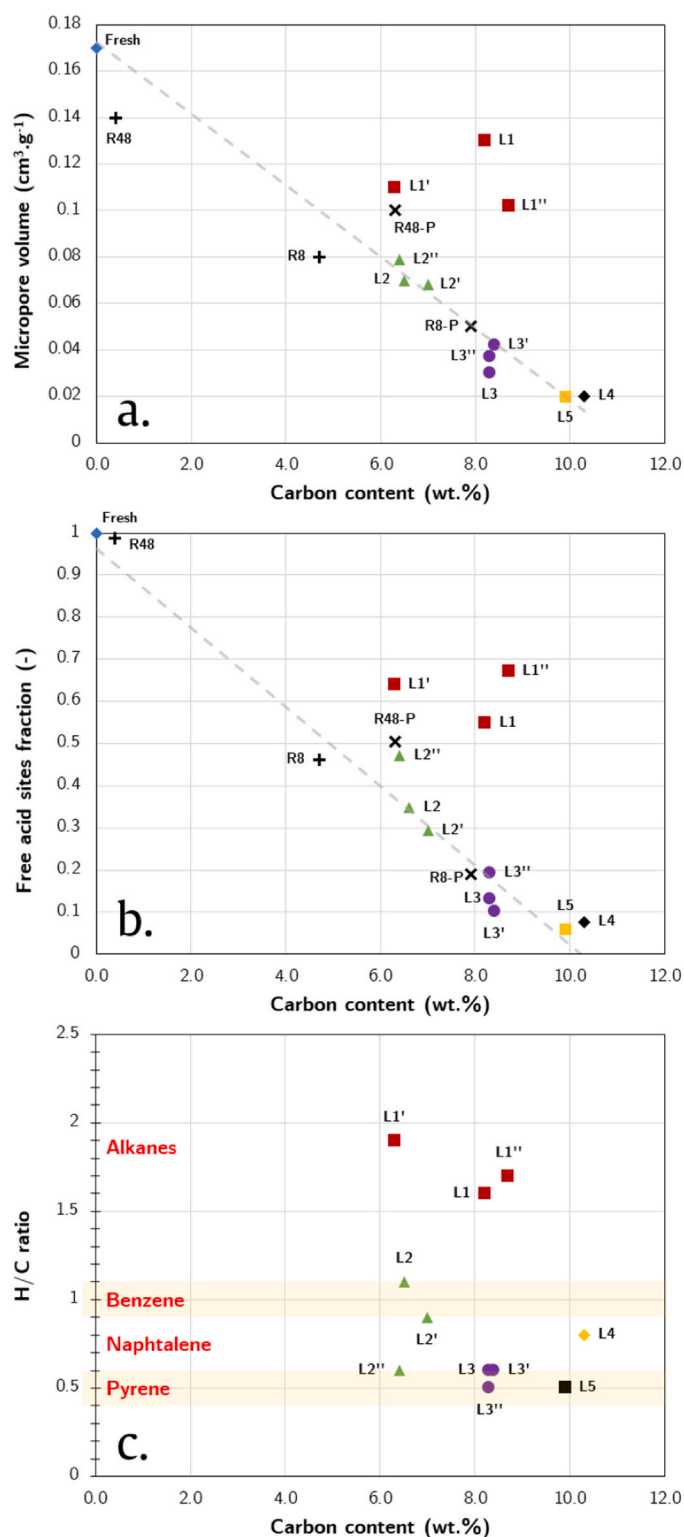


Fig. 3. Correlation between the analyzed carbon content with (a) microporosity, (b) free acid sites and (c) H/C ratio of all catalysts samples (fresh, spent, regenerated and reused). H/C ratio values superior to 1.5 are attributed to aliphatic coke. Benzene, naphthalene and pyrene-like coke structures have an H/C ratio around 1.0, 0.8 and 0.6 respectively.

abnormally high for initial experiments (L1, L1' and L1''). This important carbon deposition is attributed to the direct contact with molten polyethylene, forming a carbon-rich envelope around the pelletized catalysts or around zeolite crystals. The loading method generates heterogeneity

in coked samples due to the differences of exposition between the layers of catalysts: while three layers are mixed with LDPE, the top layer fraction is located above the plastics (Fig. 1). It is suggested that the three bottom fractions are dipped into molten polymers during the reaction while the top layer is not exposed to liquid polyethylene by staying at its surface. A different series of experiment not presented in this work, where all catalysts were placed on top of LDPE, presented lower carbon content (3.3 wt%C after one pyrolysis). The grains of this fraction are therefore exposed mainly to pyrolysis vapors, which favored diffusion leads to homogeneous coking. As the different layers cannot be collected separately, the elemental analysis might be affected by the difference of exposition. However, when furtherly reused the heterogeneity is mitigated as catalysts are mixed. After using the catalysts for the fourth and fifth times, zeolite materials seem to be saturated with coke: L4 and L5 carbon contents fluctuate around 10.0 wt% while microporous volume and acidity remain constant. Microporosity is completely either occupied or blocked, preventing any access to Brønsted acid sites. Further coke deposition can only occur in mesoporous volume by reacting with previous coke structures or remaining Lewis sites. Detailed considerations about coke location during deactivation by pyrolysis of polyethylene, as well as nature of carbonaceous structures, are discussed in the following paragraph (Section 2.1.3).

### 3.1.3. Nature and location of coke

A first approach for the determination of coke nature is provided in Fig. 3.c. The evolution of H/C ratio obtained by elemental analysis shows progressive condensation of coke structures as its value decreases when pyrolysis number increases. While H/C is around 2 for the first runs, indicating an important fraction of aliphatic coke, condensation occurs for further reuses, forming benzene-like coke (H/C  $\approx$  1), followed by naphthalene and pyrene-like molecules (H/C  $\approx$  0.5). A more precise determination of coke nature formed over ZSM-5 catalysts is determined by  $^{13}\text{C}$  NMR analysis. Obtained spectra for spent samples are presented in Fig. 4. The attribution of different observed peaks with corresponding deconvolution exploitation are presented in Table 4.

All samples present similar chemical shifts with two main domains: 18–35 ppm and 120–153 ppm. These zones are identified in the literature as aliphatic and aromatic carbons respectively [36–38]. The aromatic carbon area is the main domain observed on the NMR spectra. As sensed due to the high operating temperature of pyrolysis (450 °C), coke

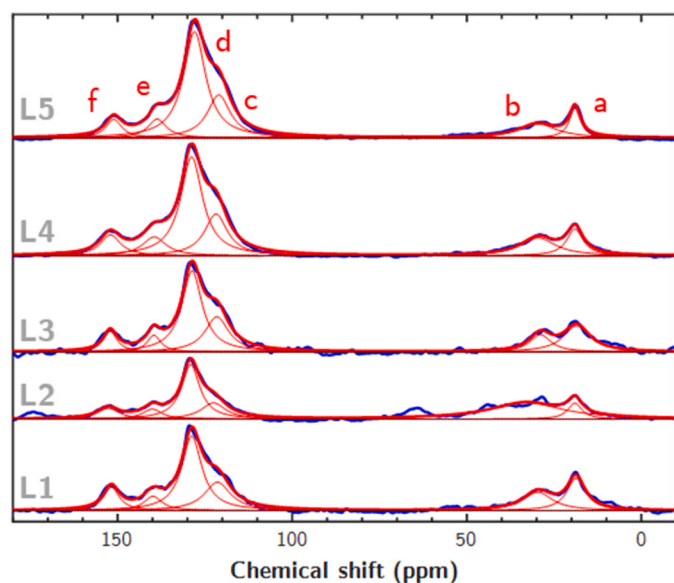
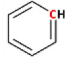
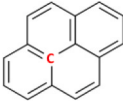
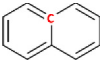
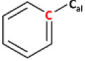


Fig. 4. Normalized  $^{13}\text{C}$  NMR spectra of the different coked samples (blue line: initial spectrum; thin red lines: deconvoluted peaks; thick red: deconvoluted spectrum; black line: baseline).

Table 4

Nature and composition of coke structures formed during pyrolysis determined by  $^{13}\text{C}$  CP-MAS NMR.

% NMR Deconvoluted Peak Area		L1	L2	L3	L4	L5
Aliphatic carbon		28.4	43.4	26.1	21.1	17.7
Methyl (18–22 ppm)	-CH <sub>3</sub>	14.9	7.0	17.0	8.7	6.8
Linear alkane (25–35 ppm)	-CH <sub>2</sub>	13.5	36.4	9.1	12.4	10.9
Aromatic carbon		71.6	56.6	73.8	78.9	82.3
Non-substituted (120–128 ppm)		18.4	12.2	20.5	18.8	20.3
3-ring junction (128–132 ppm)		37.5	30.9	40.6	43.0	48.7
2-ring junction (138–140 ppm)		6.5	6.0	5.7	8.8	7.2
Substituted (151–153 ppm)		9.2	7.5	7.1	8.3	6.1
Ratio aliphatic/aromatic		0.40	0.77	0.35	0.27	0.22
Condensation degree <sup>a</sup>		0.61	0.65	0.63	0.66	0.68

<sup>a</sup> The condensation degree is calculated as the ratio between ring junction (d, e) and total aromatic carbons.

formed is mainly heavy coke containing condensed carbons forming clusters of polyaromatics. Indeed, the two peaks attributed to ring junction (128–132 ppm and 138–140 ppm), being the most condensed form, represent the majority of aromatic carbons. The average coke structure formed is an agglomeration of condensed rings. During the successive reuses of catalysts, the condensation degree of aromatic carbons tends to increase due to the growth mechanisms of initial coke. Chen *et al.* obtained similar behavior during the catalytic pyrolysis of PE over Y-zeolite industrial catalysts in a fixed-bed [39]. The challenge of this work resides in the fact that the successive pyrolysis runs are not considered as a continuous process: both growth of initial structures and additional deposition of coke has to be considered. Every sample also presents a significant fraction of aliphatic coke (between 17.7% and 43.4%). This light coke is linear and branched alkanes or alkenes, such as partially cracked polymers or intermediate reactants that did not undergo aromatization. During PE cracking in a conical spouted bed reactor, Castaño *et al.* obtained similar mix of aliphatic and aromatic coke over HZSM-5 catalysts [48]. It is important to remind that NMR analysis are considering all coke structures regardless of their location. Indeed, coke nature and/or size is susceptible to be different according to its location within the porous matrix. Micropores are sterically limiting coke development while its growth is not restrained in mesoporous volume [49]. Location considerations therefore need to be considered to gain better insights of coke formation during pyrolysis.

Determining the repartition between internal and external coke, i.e. determining coke contained in microporous zeolite crystals and in alumina binder mesoporous volume, is a complex challenge even up to date. The external coke content is usually obtained by difference between total coke load and microporous coke. The latter is determined by correlating micropores volume loss and an approximation of coke density. However, this method approximates that all lost micro-volume is actually occupied by coke molecules which may be untrue as pore blocking can occur, especially in microporous zeolites. In this deactivation pathway, only pore mouth is covered by coke and its volume becomes inaccessible while not occupied by deactivating species. In this work, the authors intended to evaluate the contribution between actual occupancy and pore blocking in microporosity loss. The average density of coke for each sample is determined with the H/C ratio using equation

given by Kuwata *et al.* to consider the important fluctuation of coke nature confirmed by NMR analysis [50]. Calculated coke density range for all samples is between  $0.84 \text{ g}\cdot\text{cm}^{-3}$  (L1') and  $1.32 \text{ g}\cdot\text{cm}^{-3}$  (L5). This range is in accordance with the value of  $1.22 \text{ g}\cdot\text{cm}^{-3}$ , often used in the literature as value for average coke density [51,52]. Using the calculated coke density, the actual volume occupied by coke is determined with carbon mass content. The proportion of pore blocking is then calculated from the difference between this value and the apparent microporosity loss. Complete results obtained using this method are presented in Table 5. No pore blocking is observed after one pyrolysis but its contribution appears after two or more uses of catalysts (between 40% and 50%). While L5 sample shows an 88% loss of microporosity relatively to fresh zeolite, half is due to pore blockage (49.8%). This calculation considers that all coke is located in micropores. Volume occupied by mesoporous coke is here neglected due to its limited evolution. However, previous results showed that external coke has an important role in the mechanisms of coke growth and should be considered.

### 3.1.4. Conclusion on catalytic deactivation

Based on the experimental results, a comprehensive multi-step approach is proposed to describe coke formation over catalysts. Fig. 5 summarizes and illustrates this suggested deactivation pathway of ZSM-5 catalysts during pyrolysis of LDPE. The initial deactivation after the first use of catalysts in pyrolysis presents an important fraction of coke deposited at the surface of zeolite crystals (external coke). Consequently, the microporous volume and acid sites are less impacted than expected considering the coke content (Fig. 3.a and b). The high H/C ratio suggests that these deposits are mainly aliphatic compounds. The heavy coke formed during pyrolysis and exposed by NMR analysis is expected to be mostly formed in zeolite crystals (internal coke). Elordi *et al.* demonstrated similar behavior when conducting cracking of polyethylene with HZSM-5 in a conical spouted bed reactor [53]. When reusing the catalysts, further coke is deposited and carbon load increases. Mechanisms of coke growth appears on both internal and external coke: initial coke deposited in the micropores or over the surface condensates to form polyaromatic structures. The development of internal coke causes the apparition of pore blocking. Additional light coke is deposited on the crystals surface with the deposition of partially cracked polymers. This phenomenon is particularly observed after initial deactivation as reactivity is altered, enhancing aliphatic coke formation. Further reuses show typical behavior of coke growth with a gradual condensation of coke structures, surface hindering and porosity loss. At advanced stages of deactivation, the formation of a heavy coke envelope around zeolite crystals is suggested, blocking all access to microporosity and Brønsted sites. Even though part of Lewis acid sites remains available in mesoporous volume, cracking and rearrangement capacities are heavily impacted due to the important contribution of Brønsted acidity. In order to recover catalytic performances, coke has to be removed with a proper regenerating treatment. In the following section, the capacity of the ozonation process to restore catalytic performances in pyrolysis and characteristics is discussed.

**Table 5**  
Determination of pore blocking contribution in porous volume loss for the different coked samples.

Property	L1	L2	L3	L4	L5	L1'	L2'	L3'	L1''	L2''	L3''
Carbon content (wt%)	8.2	6.5	8.3	10.3	9.9	6.3	7	8.4	8.7	6.4	8.3
H/C ratio (mol/mol)	1.6	1.1	0.6	0.8	0.5	1.9	0.9	0.6	1.7	0.6	0.5
Coke density ( $\text{g}\cdot\text{cm}^{-3}$ )	0.91	1.05	1.26	1.16	1.32	0.84	1.12	1.26	0.88	1.26	1.32
Actual coke occupancy ( $\text{cm}^3$ )	0.09	0.06	0.07	0.09	0.08	0.07	0.06	0.07	0.10	0.05	0.06
Apparent coke occupancy ( $\text{cm}^3$ )	0.06	0.10	0.14	0.15	0.15	0.07	0.10	0.13	0.08	0.09	0.13
Contribution of pore blocking (%)	-	40.0	52.9	41.0	49.8	-	38.8	47.9	-	44.2	52.6

## 3.2. Ozonated catalysts efficiency and properties

Coke removal was carried out by ozonation in a fixed-bed reactor. First regenerated sample has been obtained by exposing L5 sample (9.9 wt%C) to an ozone-enriched gas stream at  $100 \text{ }^\circ\text{C}$  during 8 h (R8) to assess the ability of ozonation to remove highly condensed coke. Intending to achieve complete coke removal, ozonation in identical conditions was conducted during 48 h (R48) from a coked sample containing 5.3 wt%C. The ozonated catalysts (R8 and R48) were analyzed to measure their properties. These two regenerated samples were then recycled in two separate pyrolysis runs using the same experimental conditions as at the first pyrolysis to assess catalytic selectivity recovery. Pyrolysis products and reused zeolites were collected after reaction for analysis (R8-P and R48-P).

### 3.2.1. Study of regenerated catalysts selectivity

The compositions of pyrolysis condensed products collected after reuse of ozonated catalysts are presented in Table 2 alongside previous samples. Similarly to Section 2.1.1, the repartition of obtained oils and waxes is discussed according to their fraction (C7-C9, C10-C14 and C15 +) as well as their aromaticity. The evolution of main products, toluene and xylenes, is also presented.

The regenerating treatment applied during 8 h allowed to obtain important recovery of cracking and rearrangement performances when compared to spent catalysts capacity (L4 experiment), showing that an important part of initial catalytic selectivity is restored. While the L4 experiment presented only 27.5% of aromatics and 69.8% of light products (C7-C9), pyrolysis using R8 catalysts led to regained formation of aromatics (78.7%) and gasoline fraction (87.9%). The obtained composition is close to pyrolysis products of L1 experiment, where used catalysts were coked once, suggesting that 8 h of ozonation exposition is not sufficient to remove all deposited coke. Indeed, the lower proportions of aromatic products and C7-C9 fraction traduces the incomplete regeneration of active sites. Nevertheless, the reuse of R48 catalysts yielded pyrolysis oils with identical composition to pyrolysis with fresh catalysts, suggesting that catalytic efficiency is entirely recovered. Both aromatics and light fraction proportions are similar: 91.4% of aromatic and 92.2% of gasoline products with R48 catalysts. Similarly to combustion, complete regeneration of catalysts is difficult to achieve and require important process times. The competition of coke oxidation with ozone catalytic degradation is susceptible to extend necessary time of exposition [32]. For industrial application, an optimization of the recovery efficiency gain as a function of process time and energy consumption would be relevant. The characteristics of regenerated catalysts after the different investigated ozonation treatments are discussed in Section 2.2.2.

### 3.2.2. Catalytic properties recovery and evolution

Textural and chemical properties of regenerated and reused samples are presented in Table 6. Fresh and L5 samples characteristics are reminded for comparison purposes, being the departing samples before pyrolysis and regeneration respectively. Regenerated (R8 and R48) and reused samples (R8-P and R48-P) are included in the graphic correlation comparing microporous volume and free acid sites fraction as a function of carbon content (Fig. 3.a, b).



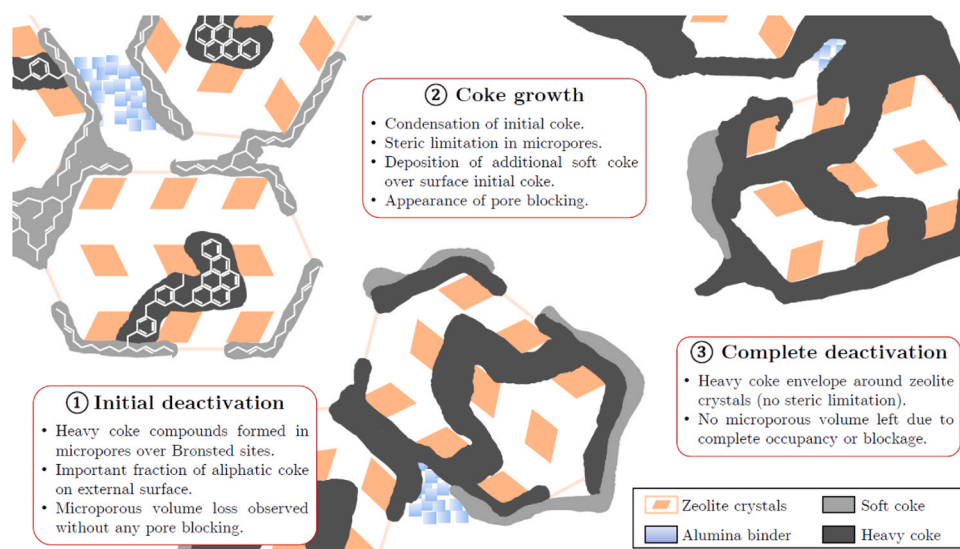


Fig. 5. Schematic representation of coke formation process in industrial ZSM-5 catalysts during successive reuses in pyrolysis of LDPE.

Table 6

Textural and chemical properties of regenerated and reused catalysts.

Property	Fresh	L5	Regenerated samples*			Reused in pyrolysis		
			R8	R48		R8-P	R48-P	
Carbon content (wt%)	-	9.9	4.7	0.4	(53%)	(92%)	7.9	6.3
BET surface area ( $\text{m}^2 \cdot \text{g}^{-1}$ )	369.6	43.3	174.3	315.6	(35%)	-	86.8	215.3
Total pore volume ( $\text{cm}^3 \cdot \text{g}^{-1}$ )	0.38	0.16	0.27	0.32	(29%)	-	0.22	0.28
Microporous volume $V_{\text{micro}}$ ( $\text{cm}^3 \cdot \text{g}^{-1}$ )	0.17	0.02	0.08	0.14	(35%)	-	0.05	0.10
Mesoporous volume $V_{\text{meso}}$ ( $\text{cm}^3 \cdot \text{g}^{-1}$ )	0.21	0.14	0.19	0.18	(24%)	-	0.17	0.18
Brønsted acid sites ( $\mu\text{mol} \cdot \text{g}^{-1}$ )	294	4	135	294	(45%)	-	50	192
Lewis acid sites ( $\mu\text{mol} \cdot \text{g}^{-1}$ )	193	25	90	187	(34%)	-	43	54

\* Fraction of removed coke and known recovery rates are indicated in gray (%) for regenerated samples. Initial coked samples properties before R48 were unknown except carbon content.

After the 8 h ozonation treatment, 53% of the initial coke is removed. As a qualitative comparison, using combustion at 550 °C during 5 h, Serrano *et al.* obtained a 64% coke removal from ZSM-5 samples coked during LDPE pyrolysis at 340 °C [20]. Characteristics of R8 sample are between those of L1 and L2 samples, such as microporous volume ( $0.08 \text{ g} \cdot \text{cm}^{-3}$ ) or Brønsted acidity ( $135 \mu\text{mol} \cdot \text{g}^{-1}$ ) for instance. Exposition time was therefore not sufficient to recover all active sites but ozonation allowed a 45% recovery for Brønsted sites and 34% of Lewis acidity. Recovery rate of mesoporous volume (24%) is less important than microporous retrieval (35%). Ozone preferentially reacts with coke located over strong acid sites in micropores. Indeed, as mentioned in Section 2.1.3, external coke for extensively coked catalysts is made mostly of very stable polyaromatic clusters while the steric limitation leads to the formation of smaller internal coke molecules. Being less stabilized by important condensation, these molecules react more easily with oxidizing agents. A difference of oxidation rate appears depending on the various structures and natures of coke molecules. The partial recovery of textural and chemical properties does not linearly correlate with the catalytic performance discussed in Section 2.2.1. Indeed, despite incomplete acid sites recovery, reuse of R-8 h sample conducted to an important catalytic efficiency of 86% regarding products aromaticity. However, residual coke is blocking a fraction of active sites. The ozonation regenerative treatment was thus applied for 48 h at 100 °C intending to achieve complete coke removal (sample R48). A coke removal of 92% is obtained, corresponding to 0.4 wt% of residual carbon. López *et al.* observed similar behavior with 0.7 wt% remaining coke (97% coke removal) after combustion treatment at 550 °C of ZSM-5 catalysts coked during plastics mix pyrolysis at 440 °C [19]. Despite

few coke remaining over R48 sample, acidity has been entirely recovered as both Brønsted and Lewis sites concentrations retrieved their initial value. The residual carbon causes partial recovery of specific surface and porosity. The fact that chemical properties are completely retrieved during ozonation suggests that ozone and/or hydroxyl radicals preferentially react with coke located over sites sites. Fraction of residual coke is located in the microporosity as only 83% of microporous volume is recovered. Such coke molecules are suggested to be inaccessible to oxidizing agents due to diffusion limitations [32].

After reuse of regenerated samples in pyrolysis, coked catalysts were collected to compare the relative deactivation rates of regenerated samples with those of initial experiments. The evolution of catalytic properties after reuse in pyrolysis is presented Fig. 6. A complete cycle is here represented: starting from fresh catalysts, followed by spent material (L5), then corresponding regenerated sample (R8) and finally after being reused in same conditions as initial pyrolysis (R8-P). The sample R48-P, obtained by reuse of R48 in pyrolysis, is also plotted for comparison and shows properties close to L1 spent catalysts. Completely regenerated and fresh catalysts therefore appear to present similar deactivation behavior. Diminution of Brønsted acid sites is identical while Lewis acidity, porosity and specific surface loss is slightly more important. Similar decrease is observed for R8-P sample, which coke content before reuse is not null (4.7 wt% C). It is expected that residual coke favor the formation of new deposits as it acts as precursors, amplifying deactivation when recycling regenerated samples with residual carbon compounds. Brønsted acidity loss between R8 and R8-P is 29% while it would be expected around 26.5% by interpolation between the samples with similar characteristics (L1 and L2). However,

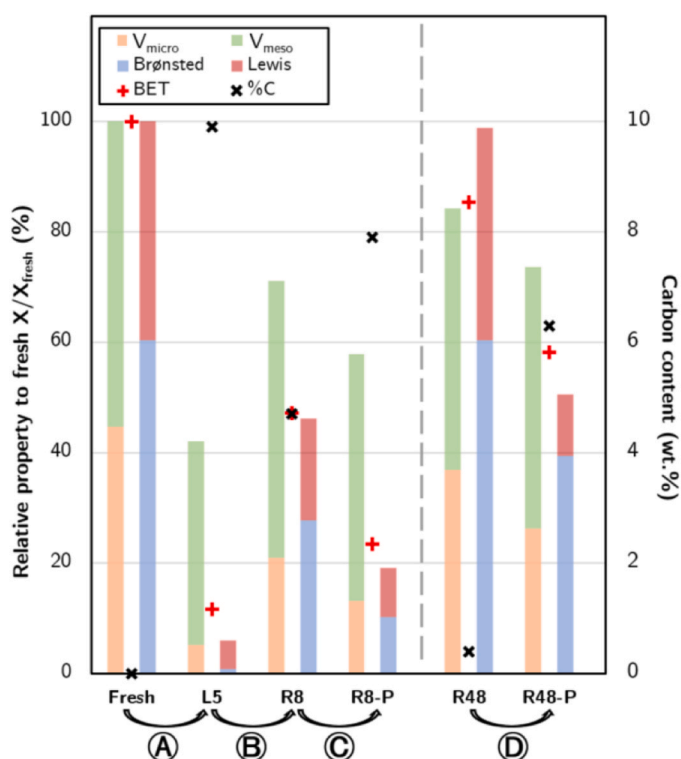


**Fig. 6.** Evolution of textural and chemical properties of catalysts samples during one cycle of pyrolysis, regeneration with different exposition times and reuse. (A: five successive pyrolysis; B: 8 h ozonation at 100 °C; C and D: reuse in pyrolysis).

comparison of relative deactivation rates is more complex and samples with exact initial characteristics would be required for accurate comparison. Based on our results, deactivation observed when reusing ozonated catalysts does not present a different rate when compared to the initial coke formation discussed in Section 2.1.2. The combined results of catalytic selectivity and zeolite material properties in this work show that ozonation is efficient in one reuse cycle. Influence of repeated regenerations, similarly to Kassargy *et al.* [31] who studied regeneration efficiency up to 14 cycles with combustion, will be investigated using ozonation and presented in a future study.

#### 4. Conclusions

The deactivation of ZSM-5 extruded catalysts during pyrolysis of low-density polyethylene at bench scale has been investigated at different levels: evolution of catalytic selectivity and textural/chemical properties. Loss of catalytic performances during successive pyrolysis is quantified with a decrease of both aromatic products and C7-C9 fraction in pyrolysis oils. Important deactivation is observed after five successive uses where collected oils present important decrease of aromatics (from 91.9 to 27.5%) and light products (from 94.9 to 69.8%). The evolution of catalysts properties combined with analysis of deactivating species nature allowed to gain better understanding of the coking process during pyrolysis of polyethylene. Microporosity is mostly impacted due to the formation of heavy coke in zeolite crystallinity and important contribution of pore blocking (around 50%). Mechanisms of coke condensation and deposition of additional external soft coke are observed until coke saturation and complete deactivation.

Coke formation is unavoidable during catalytic pyrolysis as many of the products of interest (toluene, xylenes, naphthalene) are coke precursors but irreversible. Innovative ozonation process was here investigated to remove coke and restore catalytic performance as an alternative method to coke combustion with oxygen. Regenerating

treatment with O<sub>3</sub> during 48 h in a fixed bed reactor allowed to fully recover initial catalytic selectivity and acidic properties. Pyrolysis oils obtained from ozonated catalysts reuse were similar to fresh catalysts use (91.4% aromatics, 92.2% C7-C9). Despite total acidity recovery, complete coke removal is difficult to achieve because of the ozone diffusion limitations. The preferential reactivity of ozone with microporous coke allowed to recover important proportions of initial characteristics with limited time of exposition (8 h). At moderate temperature (100 °C), ozonation can thus efficiently restore catalytic selectivity and properties of industrial ZSM-5 catalysts after one cycle of LPDE pyrolysis and regeneration. As coke formed during pyrolysis is mainly composed of heavy and stable structures, these results are promising regarding the use of ozonation in a wide range of deactivating processes with less severe deactivation conditions.

#### CRediT authorship contribution statement

**Marie-Hélène Manero:** Writing – review & editing, Validation, Supervision, Project administration, Conceptualization. **Ludovic Pinard:** Writing – review & editing, Validation, Methodology, Formal analysis, Data curation. **Valérie Ruau:** Writing – review & editing, Methodology, Formal analysis, Data curation. **Mylène Marin-Gallego:** Writing – review & editing, Methodology, Conceptualization. **Romain Richard:** Writing – review & editing, Validation, Supervision, Project administration, Methodology, Conceptualization. **Vivien Daligaux:** Writing – review & editing, Writing – original draft, Investigation, Formal analysis, Data curation.

#### Declaration of Competing Interest

The authors declare that they have no known competing financial interests or personal relationships that could have appeared to influence the work reported in this paper.

#### Data availability

Data will be made available on request.

#### Acknowledgements

The authors deeply thank T. Ménager for his important contribution to this work with the conception and manufacturing of the pyrolysis experimental setup. The authors would also like to express their gratitude to Y. Coppel and I. Borget (Laboratoire de Chimie de Coordination - UPR8241) for the implementation of the <sup>13</sup>C NMR and elemental analysis respectively. The authors also thank G. Guittier and A. Vandebossche (SAP LGC - UMR5503) for their precious help and contribution to these results with the analysis of textural catalysts properties and pyrolysis oils composition respectively. L. Pinard thanks the Région Normandie for their financial support, through the Bio/DNH project.

#### Appendix A. Supporting information

Supplementary data associated with this article can be found in the online version at [doi:10.1016/j.apcata.2024.119581](https://doi.org/10.1016/j.apcata.2024.119581).

#### References

- [1] M. Roser Hannah Ritchie, Plastic pollution, Our World Data (2018).
- [2] K. Ragaert, L. Delva, K. Van Geem, Mechanical and chemical recycling of solid plastic waste, *Waste Manag.* 69 (2017), <https://doi.org/10.1016/j.wasman.2017.07.044>.
- [3] D. Almeida, Md.F. Marques, Thermal and catalytic pyrolysis of plastic waste, *Polímeros* 26 (2016) 44–51, <https://doi.org/10.1590/0104-1428.2100>.
- [4] R. Miandad, M.A. Barakat, A.S. Aburizaiza, M. Rehan, A.S. Nizami, Catalytic pyrolysis of plastic waste: a review, *Process Saf. Environ. Prot.* 102 (2016) 822–838, <https://doi.org/10.1016/j.psep.2016.06.022>.

- [5] S.H. Gebre, M.G. Sendeku, M. Bahri, Recent trends in the pyrolysis of non-degradable waste plastics, *ChemistryOpen* 10 (2021) 1202–1226, <https://doi.org/10.1002/open.202100184>.
- [6] G. Elordi, M. Olazar, G. Lopez, M. Amutio, M. Artetxe, R. Aguado, J. Bilbao, Catalytic pyrolysis of HDPE in continuous mode over zeolite catalysts in a conical spouted bed reactor, *J. Anal. Appl. Pyrolysis* 85 (2009) 345–351, <https://doi.org/10.1016/j.jaap.2008.10.015>.
- [7] N. Zhou, L. Dai, Y. Lv, H. Li, W. Deng, F. Guo, P. Chen, H. Lei, R. Ruan, Catalytic pyrolysis of plastic wastes in a continuous microwave assisted pyrolysis system for fuel production, *Chem. Eng. J.* 418 (2021) 129412, <https://doi.org/10.1016/j.cej.2021.129412>.
- [8] M. Olazar, G. Lopez, M. Amutio, G. Elordi, R. Aguado, J. Bilbao, Influence of FCC catalyst steaming on HDPE pyrolysis product distribution, *J. Anal. Appl. Pyrolysis* 85 (2009) 359–365, <https://doi.org/10.1016/j.jaap.2008.10.016>.
- [9] M.R. Jan, J. Shah, H. Gulab, Catalytic degradation of waste high-density polyethylene into fuel products using BaCO<sub>3</sub> as a catalyst, *Fuel Process. Technol.* 91 (2010) 1428–1437, <https://doi.org/10.1016/j.fuproc.2010.05.017>.
- [10] M.S. Renzini, L.C. Lerici, U. Sedran, L.B. Pierella, Stability of ZSM-11 and BETA zeolites during the catalytic cracking of low-density polyethylene, *J. Anal. Appl. Pyrolysis* 92 (2011) 450–455, <https://doi.org/10.1016/j.jaap.2011.08.008>.
- [11] N. Miskolczi, L. Bartha, G. Deák, B. Jóver, D. Kalló, Thermal and thermo-catalytic degradation of high-density polyethylene waste, *J. Anal. Appl. Pyrolysis* 72 (2004) 235–242, <https://doi.org/10.1016/j.jaap.2004.07.002>.
- [12] A. Ochoa, J. Bilbao, A.G. Gayubo, P. Castaño, Coke formation and deactivation during catalytic reforming of biomass and waste pyrolysis products: a review, *Renew. Sust. Energ. Rev.* 119 (2020) 109600, <https://doi.org/10.1016/j.rser.2019.109600>.
- [13] M. Guisnet, P. Magnoux, Organic chemistry of coke formation, *Appl. Catal. A* 212 (2001) 83–96, [https://doi.org/10.1016/S0926-860X\(00\)00845-0](https://doi.org/10.1016/S0926-860X(00)00845-0).
- [14] M. Guisnet, L. Costa, F.R. Ribeiro, Prevention of zeolite deactivation by coking, *J. Mol. Catal. A Chem.* 305 (2009) 69–83, <https://doi.org/10.1016/j.molcata.2008.11.012>.
- [15] G. Elordi, M. Olazar, G. Lopez, P. Castaño, J. Bilbao, Role of pore structure in the deactivation of zeolites (HZSM-5, H $\beta$  and HY) by coke in the pyrolysis of polyethylene in a conical spouted bed reactor, *Appl. Catal. B* 102 (2011) 224–231, <https://doi.org/10.1016/j.apcatb.2010.12.002>.
- [16] M. Argyle, C. Bartholomew, Heterogeneous catalyst deactivation and regeneration: a review, *Catalysts* 5 (2015) 145–269, <https://doi.org/10.3390/catal5010145>.
- [17] J. Zhou, J. Zhao, J. Zhang, T. Zhang, M. Ye, Z. Liu, Regeneration of catalysts deactivated by coke deposition: a review, *Chin. J. Catal.* 41 (2020) 1048–1061, [https://doi.org/10.1016/S1872-2067\(20\)63552-5](https://doi.org/10.1016/S1872-2067(20)63552-5).
- [18] A. Marcilla, M.I. Beltrán, R. Navarro, Effect of regeneration temperature and time on the activity of HUSY and HZSM5 zeolites during the catalytic pyrolysis of polyethylene, *J. Anal. Appl. Pyrolysis* 74 (2005) 361–369, <https://doi.org/10.1016/j.jaap.2004.10.006>.
- [19] A. López, I. de Marco, B.M. Caballero, A. Adrados, M.F. Laresgoiti, Deactivation and regeneration of ZSM-5 zeolite in catalytic pyrolysis of plastic wastes, *Waste Manag.* 31 (2011) 1852–1858, <https://doi.org/10.1016/j.wasman.2011.04.004>.
- [20] D.P. Serrano, J. Aguado, J.M. Rodríguez, A. Peral, Catalytic cracking of polyethylene over nanocrystalline HZSM-5: catalyst deactivation and regeneration study, *J. Anal. Appl. Pyrolysis* 79 (2007) 456–464, <https://doi.org/10.1016/j.jaap.2006.11.013>.
- [21] V. Daligaux, R. Richard, M.-H. Manero, Deactivation and regeneration of zeolite catalysts used in pyrolysis of plastic wastes—a process and analytical review, *Catalysts* 11 (2021) 770, <https://doi.org/10.3390/catal11070000>.
- [22] L.Y. Jia, A. Farouha, L. Pinard, S. Hedan, J.D. Comparot, A. Dufour, K. Ben Tayeb, H. Vezin, C. Batiot-Dupeyrat, New routes for complete regeneration of coked zeolite, *Appl. Catal. B* 219 (2017) 82–91, <https://doi.org/10.1016/j.apcatb.2017.07.040>.
- [23] R. Richard, C. Julcour, M. Manero, Towards a new oxidation process using ozone to regenerate coked catalysts, *Ozone Sci. Eng.* 39 (2017) 366–373, <https://doi.org/10.1080/01919512.2017.1326005>.
- [24] M.V. Morales, K. Góra-Marek, H. Musch, A. Pineda, B. Murray, S. Stefanidis, L. Falco, K. Tarach, E. Ponomareva, J.H. Marsman, I. Melián-Cabrera, Advanced oxidation process for coke removal: a systematic study of hydrogen peroxide and OH-derived-Fenton radicals of a fouled zeolite, *Appl. Catal. A* 562 (2018) 215–222, <https://doi.org/10.1016/j.apcata.2018.06.008>.
- [25] L. Pinard, N. Ayoub, C. Batiot-Dupeyrat, Regeneration of a coked zeolite via nonthermal plasma process: a parametric study, *Plasma Chem. Plasma Process.* 39 (2019) 929–936, <https://doi.org/10.1007/s11090-019-09972-x>.
- [26] M.-C. Silaghi, C. Chizallet, J. Sauer, P. Raybaud, Dealumination mechanisms of zeolites and extra-framework aluminum confinement, *J. Catal.* 339 (2016) 242–255, <https://doi.org/10.1016/j.jcat.2016.04.021>.
- [27] S. Khangkham, C. Julcour-Lebigue, S. Damronglerd, C. Ngamcharussrivichai, M.-H. Manero, H. Delmas, Regeneration of coked zeolite from PMMA cracking process by ozonation, *Appl. Catal. B* 140–141 (2013) 396–405, <https://doi.org/10.1016/j.apcatb.2013.04.041>.
- [28] S.D. Anuar Sharuddin, F. Abnisa, W.M.A. Wan Daud, M.K. Aroua, A review on pyrolysis of plastic wastes, *Energy Convers. Manag.* 115 (2016) 308–326, <https://doi.org/10.1016/j.enconman.2016.02.037>.
- [29] S. Budsaereechai, A.J. Hunt, Y. Ngernyen, Catalytic pyrolysis of plastic waste for the production of liquid fuels for engines, *RSC Adv.* 9 (2019) 5844–5857, <https://doi.org/10.1039/C8RA10058F>.
- [30] M. Díaz, E. Epelde, J. Valecillos, S. Izaddoust, A.T. Aguayo, J. Bilbao, Coke deactivation and regeneration of HZSM-5 zeolite catalysts in the oligomerization of 1-butene, *Appl. Catal. B* 291 (2021) 120076, <https://doi.org/10.1016/j.apcatb.2021.120076>.
- [31] C. Kassargy, S. Awad, G. Burnens, G. Upreti, K. Kahine, M. Tazerout, Study of the effects of regeneration of USY zeolite on the catalytic cracking of polyethylene, *Appl. Catal. B* 244 (2019) 704–708, <https://doi.org/10.1016/j.apcatb.2018.11.093>.
- [32] V. Daligaux, R. Richard, M.H. Manero, Regeneration of coked catalysts via ozonation: experimental study of diffusion–reaction mechanisms at pellet and reactor scales, *Chem. Eng. J.* 476 (2023) 146446, <https://doi.org/10.1016/j.cej.2023.146446>.
- [33] Horv Aacute, G. Th, Eacute Za, K. Kawazoe, Method for the calculation of effective pore size distribution in molecular sieve carbon, *J. Chem. Eng. Jpn.* 16 (1983) 470–475, <https://doi.org/10.1252/jcej.16.470>.
- [34] C.A. Emeis, Determination of integrated molar extinction coefficients for infrared absorption bands of pyridine adsorbed on solid acid catalysts, *J. Catal.* 141 (1993) 347–354, <https://doi.org/10.1006/jcat.1993.1145>.
- [35] P. Duan, K. Schmidt-Rohr, Composite-pulse and partially dipolar dephased multiCP for improved quantitative solid-state <sup>13</sup>C NMR, *J. Magn. Reson.* 285 (2017) 68–78, <https://doi.org/10.1016/j.jmr.2017.10.010>.
- [36] T. Thonhauser, D. Ceresoli, N. Marzari, NMR shifts for polycyclic aromatic hydrocarbons from first-principles, *Int. J. Quantum Chem.* 109 (2009) 3336–3342, <https://doi.org/10.1002/qua.21941>.
- [37] Y. Ruiz-Morales, A.D. Miranda-Olvera, Bn Portales-Martínez, J.M. Domínguez, Determination of <sup>13</sup>C NMR chemical shift structural ranges for polycyclic aromatic hydrocarbons (PAHs) and PAHs in asphaltenes: an experimental and theoretical density functional theory study, *Energy Fuels* 33 (2019) 7950–7970, <https://doi.org/10.1021/acs.energyfuels.9b00182>.
- [38] J. Pan, G. Liao, R. Su, S. Chen, Z. Wang, L. Chen, L. Chen, X. Wang, Y. Guo, <sup>13</sup>C solid-state NMR analysis of the chemical structure in petroleum coke during idealized in situ combustion conditions, *ACS Omega* 6 (2021) 15479–15485, <https://doi.org/10.1021/acsomega.1c02055>.
- [39] Z. Chen, X. Zhang, F. Yang, H. Peng, X. Zhang, S. Zhu, L. Che, Deactivation of a Y-zeolite based catalyst with coke evolution during the catalytic pyrolysis of polyethylene for fuel oil, *Appl. Catal. A* 609 (2021) 117873, <https://doi.org/10.1016/j.apcata.2020.117873>.
- [40] R.K. Singh, B. Ruj, A.K. Sadhukhan, P. Gupta, V.P. Tigga, Waste plastic to pyrolytic oil and its utilization in CI engine: performance analysis and combustion characteristics, *Fuel* 262 (2020) 116539, <https://doi.org/10.1016/j.fuel.2019.116539>.
- [41] J. Aguado, D.P. Serrano, J.L. Sotelo, R. Van Grieken, J.M. Escola, Influence of the operating variables on the catalytic conversion of a polyolefin mixture over HMCM-41 and nanosized HZSM-5, *Ind. Eng. Chem. Res.* 40 (2001) 5696–5704, <https://doi.org/10.1021/ie010420c>.
- [42] S. Papuga, M. Djurdjevic, A. Ciccio, S. Vecchio Cipriotti, Catalytic pyrolysis of plastic waste and molecular symmetry effects: a review, *Symmetry* 15 (2023) 38, <https://doi.org/10.3390/sym15010038>.
- [43] A.C.S. Serra, J.V. Milato, J.G. Faillace, M.R.C.M. Calderari, Reviewing the use of zeolites and clay based catalysts for pyrolysis of plastics and oil fractions, *Braz. J. Chem. Eng.* 40 (2023) 287–319, <https://doi.org/10.1007/s43153-022-00254-2>.
- [44] D. Zhao, X. Wang, J.B. Miller, G.W. Huber, The chemistry and kinetics of polyethylene pyrolysis: a process to produce fuels and chemicals, *ChemSusChem* 13 (2020) 1764–1774, <https://doi.org/10.1002/cssc.201903434>.
- [45] B. Liu, D. Slocombe, M. AlKinany, H. AlMegren, J. Wang, J. Arden, A. Vai, S. Gonzalez-Cortes, T. Xiao, V. Kuznetsov, P.P. Edwards, Advances in the study of coke formation over zeolite catalysts in the methanol-to-hydrocarbon process, *Appl. Petrochem. Res.* 6 (2016) 209–215, <https://doi.org/10.1007/s13203-016-0156-z>.
- [46] G.L. Woolery, G.H. Kuehl, H.C. Timken, A.W. Chester, J.C. Vartuli, On the nature of framework Brønsted and Lewis acid sites in ZSM-5, *Zeolites* 19 (1997) 288–296, [https://doi.org/10.1016/S0144-2449\(97\)00086-9](https://doi.org/10.1016/S0144-2449(97)00086-9).
- [47] A. Corma, J. Planellas, J. Sánchez-Marín, F. Tomás, The role of different types of acid site in the cracking of alkanes on zeolite catalysts, *J. Catal.* 93 (1985) 30–37, [https://doi.org/10.1016/0021-9517\(85\)90148-4](https://doi.org/10.1016/0021-9517(85)90148-4).
- [48] P. Castaño, G. Elordi, M. Olazar, A. Aguayo, B. Pawelec, J. Bilbao, Insights into the coke deposited on HZSM-5, H beta and HY zeolites during the cracking of polyethylene, *Appl. Catal. B* 104 (2011) 91–100, <https://doi.org/10.1016/j.apcatb.2011.02.024>.
- [49] M. He, M.-F. Ali, Y.-Q. Song, X.-L. Zhou, J.A. Wang, X.-Y. Nie, Z. Wang, Study on the deactivation mechanism of HZSM-5 in the process of catalytic cracking of n-hexane, *Chem. Eng. J.* 451 (2023) 138793, <https://doi.org/10.1016/j.cej.2022.138793>.
- [50] M. Kuwata, S.R. Zorn, S.T. Martin, Using elemental ratios to predict the density of organic material composed of carbon, hydrogen, and oxygen, *Environ. Sci. Technol.* 46 (2012) 787–794, <https://doi.org/10.1021/es202525q>.
- [51] D.M. Bibby, N.B. Milestone, J.E. Patterson, L.P. Aldridge, Coke formation in zeolite ZSM-5, *J. Catal.* 97 (1986) 493–502, [https://doi.org/10.1016/0021-9517\(86\)90020-5](https://doi.org/10.1016/0021-9517(86)90020-5).
- [52] M. Choi, K. Na, J. Kim, Y. Sakamoto, O. Terasaki, R. Ryoo, Stable single-unit-cell nanosheets of zeolite MFI as active and long-lived catalysts, *Nature* 461 (2009) 246–249, <https://doi.org/10.1038/nature08288>.
- [53] G. Elordi, M. Olazar, M. Artetxe, P. Castaño, J. Bilbao, Effect of the acidity of the HZSM-5 zeolite catalyst on the cracking of high density polyethylene in a conical spouted bed reactor, *Appl. Catal. A* 415–416 (2012) 89–95, <https://doi.org/10.1016/j.apcata.2011.12.011>.